Arab J Sci Eng (2015) 40:2447–2455
DOI 10.1007/s13369-015-1647-4

RESEARCH ARTICLE - CIVIL ENGINEERING

Strength and Physico-chemical Characteristics of Fly Ash–Bottom Ash Mixture

Nima Latifi[1] · **Aminaton Marto**[1] · **Ahmad Safuan A. Rashid**[1] · **Jacky Ling Jia Yii**[1]

Received: 11 October 2014 / Accepted: 26 March 2015 / Published online: 9 April 2015

Abstract The quantity of coal combustion products, particularly fly ash (FA) and bottom ash (BA), has been increasing from coal power plants around the world. The major problem of a coal combustion-based power plant is that it produces huge quantities of solid waste. Recently, there have been efforts to use FA and BA together as a mixture in construction works. This paper investigates morphology and chemical and strength characteristics of an FA–BA mixture for various curing periods. Scanning electron microscopy (SEM), X-ray fluorescence (XRF), and consolidated undrained triaxial tests were used to determine the physico-chemical characteristics of the mixture. Based on SEM results, it was found that, with an increasing ratio of BA to FA, the number of irregular particles in the mixture increased. The results of XRF indicated noticeable changes in the surface composition of both FA and BA particles after mixing. The physico-chemical test results indicate the formation of a new gel form product in the mixture, which has been identified as calcium silicate hydrate (C-S-H). From an engineering point of view, the results indicated that the value of modulus of elasticity decreases with increasing BA content, from 30 to 70 %, in the ash mixture. However, the increase in BA from 30 to 70 % did not have any significant effect on the shear strength of the FA–BA mixture.

Keywords Fly ash (FA) · Bottom ash (BA) · Morphology · SEM · Modulus of elasticity

✉ Nima Latifi
En_Latifi@yahoo.com

[1] Geotechnic and Transportation Department, Faculty of Civil Engineering, Universiti Teknologi Malaysia (UTM), 81310 Skudai, Johor, Malaysia

1 Introduction

The major problem of coal combustion products (CCPs) is the production of large quantities of solid waste. The CCPs include silica (61 %), alumina (22 %) and iron oxide (7 %), which make up to 90 % of the ash. The other elements are calcium (Ca), magnesium (Mg), sodium (Na), potassium (K) and sulphur (S) [1]. The quantity of CCP, particularly fly ash and bottom ash, has been increasing from the coal power plants around the world. The ash collected at the bottom of the boiler—the so-called bottom ash—is of coarse grain size, unlike the fine-sized fly ash [2]. Fly ash and bottom ash being industrial wastes, if not utilized suitably, have to be disposed off in landfill, ponds or rivers. However, since they are produced in large volumes as a residual matter, their disposal may result in serious environmental problems. For example, India produces about 100 million tons of Portland cement annually. Nevertheless, it also generates 100 million tons of fly ash annually [3].

In recent years, the cost of disposing of CCPs has been a cause for concern. Hence, engineers are forced to seek alternatives to take advantage of these coal solid wastes. Coal-burning power plants produce a large volume of coal ash and bottom ash [4]. Most of the CCPs are disposed off as slurry into ash ponds, owing to low operation costs and easy operation. The solid CCPs are collected and mixed with water, and the slurry is pumped through a series of pressurized pipes into ash ponds [5]. In recent years, some studies have been conducted to identify the CCPs' physical and chemical properties [6,7]. The chemical composition in fly ash depends mainly on the chemical properties of the coal burned. In addition, it is also affected by the grinding equipment, furnace, combustion process, and nitrogen oxide control equipment used. The key factor in determining its potential use in manufactur-

ing and construction applications is the properties of fly ash [8].

Fly ash is a type of pozzolan material and has the ability of undergoing pozzolanic activity [9,10]. In pozzolanic activities, when fly ash is added with water, the active chemical components such as silica, SiO_2, and alumina Al_2O_3 will react with calcium hydroxide, $Ca(OH)_2$. The product of both active components and $Ca(OH)_2$ leads to the formation of new cementitious products, which depend on the majority of the elements inside. The latter is called the pozzolanic process, which is time-consuming [11,12]. The pozzolanic reaction is similar to the hardening of cement, so it reacts to the same types of hardening accelerators and retarders that are used in Portland cement applications [13–16].

In recent years, some studies have been conducted to utilize the fly and bottom ash mixture as a replacement material in geotechnical works, such as road and embankment construction [17–20]. In addition, the results of previous studies have indicated that the geotechnical properties of fly ash, such as specific gravity, permeability, consolidation characteristics, and internal friction angle, indicate that the material is appropriate for embankments and structural fills [13,15]. It is well established that the properties of fly ash enhance good bearing support, with minimal settlement, and fly ash is a suitable material for placement over low bearing strength and soft soil, owing to its low unit weight. Readily available fly ash can be compacted layer by layer, to achieve the level of compaction needed using the respective moisture content obtained from a compaction test. Thus, construction time and cost can be reduced [2,10].

On the other hand, previous studies indicated that bottom ash has particles that are coarser than those of fly ash and can be used in structural fills, road base, or sub-base applications, as well as fine aggregate in asphalt paving mixtures [21]. It should be noted that the range of particle size for bottom ash is from 10 to 0.075 mm, which means from fine gravel to fine sand sizes. The dry bottom ash has specific gravity around 2.0–2.6, while the specific gravity for boiler slag ranges from 2.6 to 2.9 [22]. It was reported by other researchers that, because of bottom ash properties, there are many benefits of using it in various geotechnical and material engineering works [23,24].

Prior studies indicated that the Tanjung Bin power plant in Johor, a state in southern Malaysia, produces 180 tons per day of bottom ash and 1620 tons per day of fly ash, from burning 18,000 tons of coal per day alone [21]. In addition, it was found that the major chemical composition of bottom ash in the coal power plants in Tanjung Bin in Johor was silica (SiO_2), alumina (Al_2O_3), iron oxide (Fe_2O_3), and calcium oxide (CaO) [20].

Generally, in Malaysia, the study of the coal ash and bottom ash mixture and its physico-chemical characteristics are limited, and a clear lack of understanding, regarding the morphology, chemical composition, and strength assessment of the fly ash and bottom ash mix design, is apparent.

Also, the appropriate proportion of fly ash and bottom ash mixtures is also important to maximize the strength of the mixture. Hence, this paper has made an effort to recognize the morphology changes, chemical composition, and strength assessment of fly ash and bottom ash mixtures for various curing periods. The used tests were scanning electron microscopy (SEM), energy-dispersive X-ray spectrometry (EDAX), X-ray fluorescence (XRF), and consolidated undrained (CU) triaxial.

Table 1 Physical characteristics and chemical composition of the FA and BA

Physical properties and chemical composition	Values	
	FA	BA
pH ($L/S = 2.5$)	8.57	8.44
Specific gravity	2.19	236
Optimum moisture content (%)	19	24
Maximum dry density ($mg\,m^{-3}$)	1.56	1.14
BS classification	ML	SW-SM
Coefficient of permeability (m/s)	2.86×10^{-7}	6.88×10^{-6}
CO_2 (%)	0.10	0.10
SiO_2 (%)	40.08	46.60
Al_2O_3 (%)	18.81	23.61
Fe_2O_3 (%)	17.7	12.40
CaO (%)	14.32	11.31
TiO_2 (%)	4.44	1.84
K_2O (%)	1.84	1.34
MgO (%)	1.52	1.26
P_2O_5 (%)	0.37	0.62
Na_2O (%)	0.72	0.62
SO_3 (%)	0.1	0.30
SrO (%)	1.63	0.19
BaO (%)	0.85	0.13

2 Materials and Experimental Programme

2.1 Materials

The FA and the BA were prepared at the Tanjung Bin power plant, Johor, Malaysia. Table 1 presents the physical and chemical properties of the selected FA and BA. The table shows that the FA and the BA consist mainly of silica, alumina, ferric oxide, and calcium oxide. The X-ray diffraction (XRD) result, shown in Figs. 1 and 2, indicates that the main minerals present in the FA and BA are mullite, quartz, calcite, and haematite [25]. The BA that was taken from the power plant was wet, while the fly ash was dry. All the FA

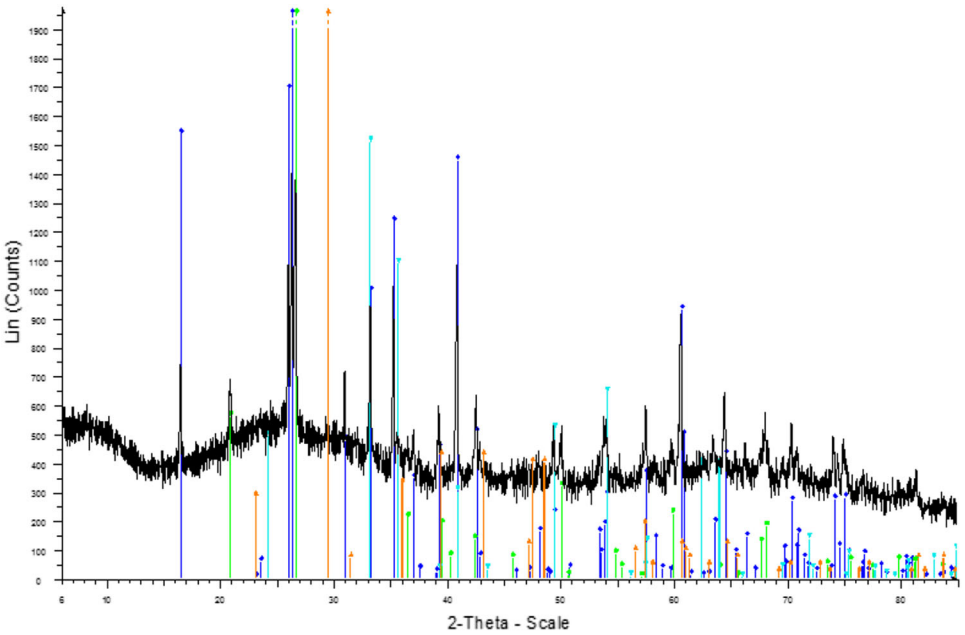

Fig. 1 XRD pattern of FA

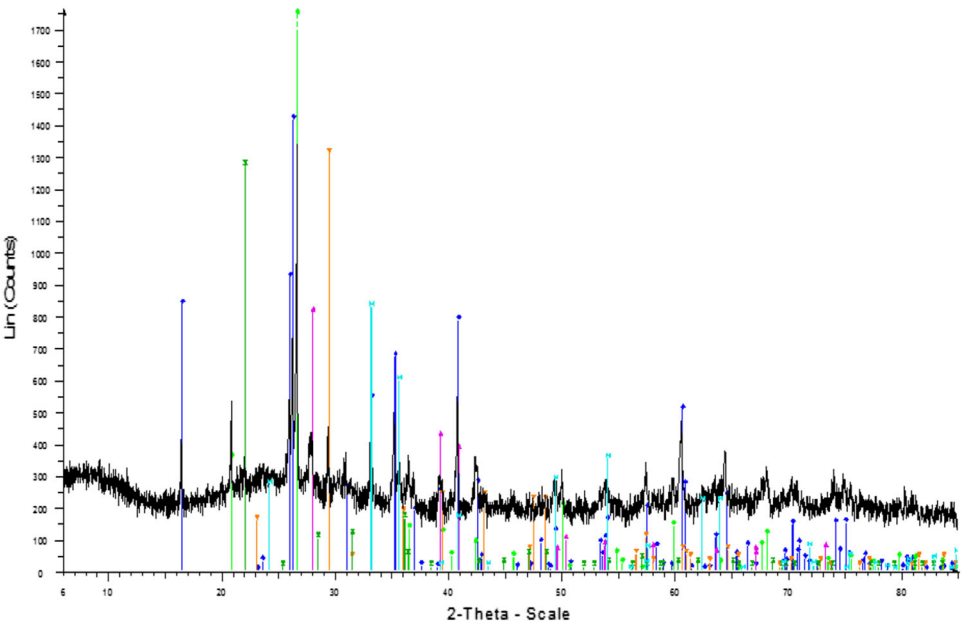

Fig. 2 XRD pattern of BA

and the BA were kept in a box after they were taken from the power plant, to prevent the materials from being exposed to the environment. The bottom ash was sieved by a No. 200 sieve and dried in the oven for 24 h, to get rid of the moisture in the bottom ash sample [26].

3 Sample Preparation and Testing Program

In this study, the BA was mixed with different proportions of FA, which were 30 % BA:70 % FA as the high amount of FA content, and 70 % BA:30 % FA as the high amount of BA. With this aim, the FA and the BA were sieved by a 2 mm mesh to confirm the uniformity of the materials [27]. In order to prepare two mix designs, a standard protocol was used. The first step was conducted based on clause 3.3.4.2 of BS 1377: Part 4: British Standards Institution (1990a). This step included the determination of the optimum moisture content and maximum dry density for FA and BA mixtures [20]. To prepare a homogeneous sample, irregular hand-mixing with palette knives was done. Subsequently, the desired dry density and the moisture content were reached by compressing the samples in a steel cylindrical mould, fitted with a collar that accommodated all the mixtures. The required compaction was done by a hydraulic jack using persistent compaction, based on clause 4.1.5 of BS 1924: Part 2: British Standards

Institution (1990b). The cylindrical samples were extruded using a steel plunger. They were then trimmed, cleaned of releasing oil, placed in a plastic bottle, and wrapped in several runs of cling film. These samples were used for the tests immediately after preparation (0 day curing) and after cured for 28 days in a temperature-controlled room [28].

The strength improvement index was determined by a consolidated undrained triaxial compression shear test (CU) at various curing periods. To do this, the specimens were placed under three different confining pressures (100, 200, and 400 kPa), and the strain rates of 0.05 % per min was chosen as that adopted by Head and Epps (1980). After the specimens had been cured, they were tested on an electron microscopic and an XRF machine. The morphology of the mixture was then tested by using a SEM machine. A JSM-6380LA JEOL scanning electron microscope machine equipped with energy-dispersive X-ray spectrometry (EDAX) was used in this study. It should be noted that the sample preparation for SEM analysis involved drying the samples and placing them onto an aluminium stub, covered with double-sided carbon tape, and coating the specimen with platinum, using a vacuum sputter coater, in order to prevent surface charging and loss of resolution. X-ray fluorescence is a technique to analyse and determine the major material elements and chemical components of mixtures. In addition, it can be used to carry out a wide ranging elemental survey of the composition of samples. The samples were prepared in a size of 20–50 mm in dry conditions. Then, a Bruker AXS Model S4 Pionner was used to identify the chemical content of the samples.

4 Results and Discussion

The SEM was used to analyse the morphology characteristics of the BA and FA mixtures, to characterize the shape and surface texture of the mixtures particles, and to gain some insight into the behaviour of the mixtures. Figures 3 and 4 present the electron micrographs of three different proportions of ash mixture, with two different curing periods. 0 % BA samples, indicating that they were 100 % FA, were used as the control sample. Initially, at day 0, it was found that the texture of FA was glassy, well rounded, and spherical in shape; there were numbers of irregularly shaped particles and smooth particle surfaces. As the portion of BA increased in the samples, which were 30 and 70 % BA, the number of irregularly shaped particles also increased. This was because BA had irregular shape, was rough, and had gritty textural surface. However, BA's surface was still shiny, clean, and dust free.

The electron micrographs of the samples for 28 days of curing period are shown in Fig. 4. The micrographs indicated that after 28 days of curing, the shapes of the fly ash and bottom ash were coarser, as a result of the pozzolanic reaction, and the numbers of irregular shapes increased [11].

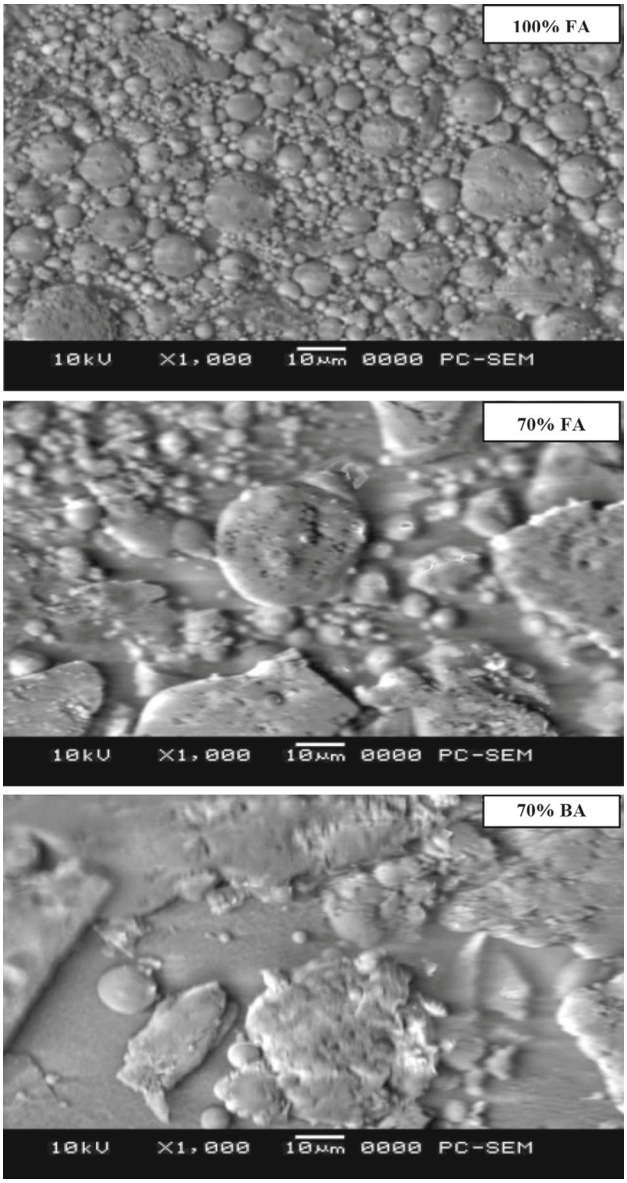

Fig. 3 SEM micrographs of coal ash mixtures particles from Tanjung Bin power plant at 0-day curing period

There were also some agglomerate-bonded particles caused by crystal growth and pozzolanic activities. The agglomerate forms ranged from lightly cemented to strongly bonded. In addition, based on the SEM results after a 28-day curing period, it was found that the size of FA also increased when the curing period increased [7]. The pozzolanic reaction products were formed when water was added to the FA and the BA mixture. The formation of resultant products was different with a variety of ash mixtures. The new products formed decreased with the BA content in the mixture. The gels bonded the ash particles together and the bonding increased with curing time. When the particles became coarser, owing to the reaction that had occurred, the rough surface of the particle reduced the movement between them,

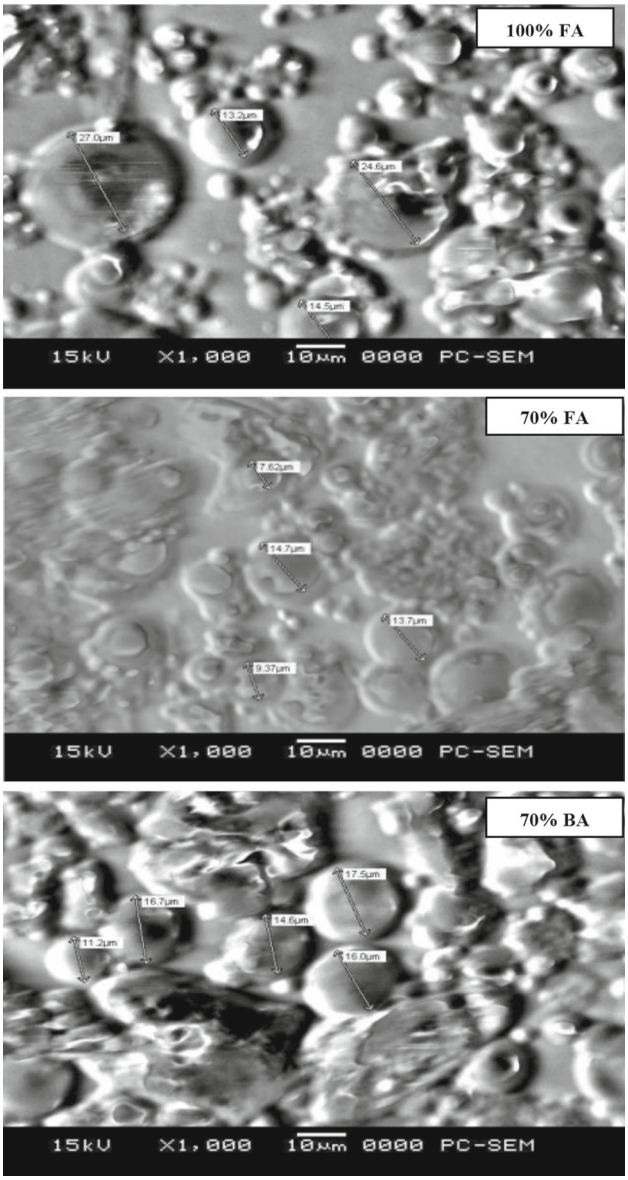

Fig. 4 SEM micrographs of coal ash mixtures particles from Tanjung Bin power plant after 28-day curing periods

which affected the particle interlocking. Thus, the strength of the mixtures increased as the duration of curing of the mixture increased. It should also be noted that by using an energy-dispersive X-ray spectrometer (EDAX) technique, this compound was roughly identified as calcium silicate hydrate (C-S-H) [29].

It is well established that fly ash consists of a high percentage of silica, alumina, and calcium [29]. In order to better understand the surface composition of treated particles, the time-dependent variations in the ratios of SiO_2/Al_2O_3 and CaO/Al_2O_3 for different mix designs, obtained from XRF results analysis, are shown in Tables 2 and 3. The comparison of the results revealed a noticeable change in the surface composition of both FA and BA particles after mixing. Tables 2 and 3 show that both SiO_2/Al_2O_3 and CaO/Al_2O_3 reduced with curing periods. Based on the elemental composition of FA and BA (SiO_2 is the dominant element in both of them), the silica layer placed at the surface had reacted with the calcium, causing the reduction in the SiO_2/Al_2O_3 ratio of the mixtures. For the CaO/Al_2O_3 ratios in particular, there was a significant reduction in the ratio of the mixed samples with increased curing time. The latter was a result of the consumption of calcium when reacting in the mixtures, in the newly formed cementing product, which was identified as C-S-H [7,11,30].

The results of the CU tests indicated that the graph of deviator stress versus axial strain and pore water pressure changed with axial strain for two different specimens, of 70 % FA and 70 % BA. The specimens were compacted with a relative compaction level of 95 % and sheared in a triaxial undrained condition for three different confining stresses, i.e., 100, 200, and 400 kPa. It can be observed that in both samples, as the deviator stress, q, increased, the pore water pressure increased too. The peak strength of the samples was the maximum value of deviator stress. The deviator stress of the critical state occurred when the pore water pressure was constant. If compared to the response of 70 % BA to 70 % FA mixtures, the peak deviator stress increased with the increase in dilation of pore water pressure. Figure 5a, b indicates that the curing period of samples and confining stress, σ_3, also affect the deviator stress and the pore water pressure at a critical state. For example, for a specimen with 70 % BA content, the deviator stress is at critical for a confining pressure of 100,

Table 2 SiO_2/Al_2O_3 and CaO/Al_2O_3 ratios of 70 % FA:30 % BA mixture at various curing time obtained from XRF analysis

100 % FA	FA and BA mixture—0 days	FA and BA mixture—28 days
$SiO_2/Al_2O_3 = 2.13$	$SiO_2/Al_2O_3 = 2.00$	$SiO_2/Al_2O_3 = 1.69$
$CaO/Al_2O_3 = 0.76$	$CaO/Al_2O_3 = 0.43$	$CaO/Al_2O_3 = 0.38$

Table 3 SiO_2/Al_2O_3 and CaO/Al_2O_3 ratios of 70 % BA:30 % FA mixture at various curing time obtained from XRF analysis

100 % BA	BA and FA mixture—0 days	BA and FA mixture—28 days
$SiO_2/Al_2O_3 = 1.97$	$SiO_2/Al_2O_3 = 1.63$	$SiO_2/Al_2O_3 = 1.31$
$CaO/Al_2O_3 = 0.47$	$CaO/Al_2O_3 = 0.36$	$CaO/Al_2O_3 = 0.27$

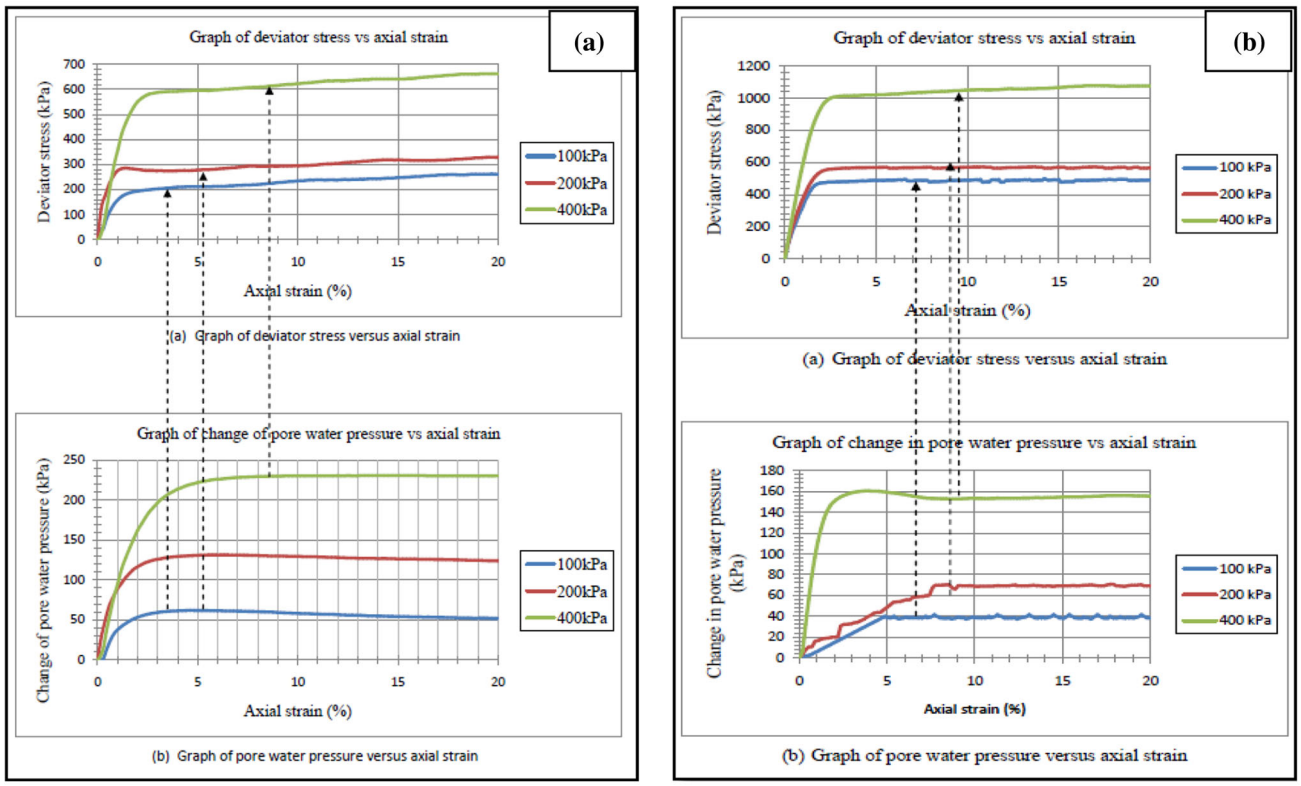

Fig. 5 Consolidated undrained compression test results for normally consolidated 70 % BA samples **a** 0 day of curing, **b** 28 days of curing

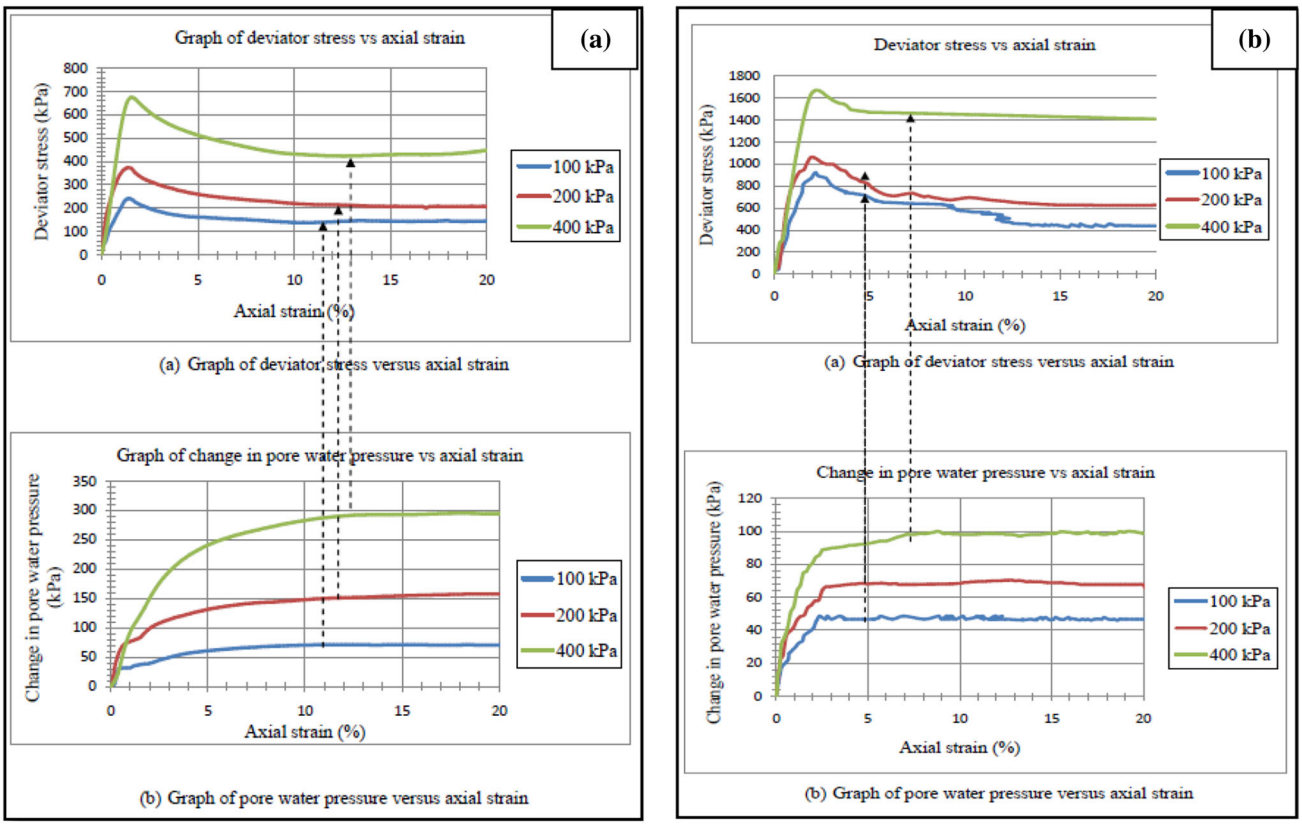

Fig. 6 Consolidated undrained compression test results for normally consolidated 70 % FA samples **a** 0 day of curing, **b** 28 days of curing

200, and 400 kPa, and corresponding effective consolidation pressures were at 208, 278, and 614 kPa, respectively. The pore water pressure was directly proportional to the increasing effective confining pressure.

After curing for 28 days, the deviator stress at critical state had increased to 478, 563, and 1026 kPa, respectively, with the effective consolidation pressure of 100, 200, and 400 kPa. For the 70 % FA specimen, Fig. 6a, b shows that the higher the effective confining pressure, the higher the deviator stress will ultimately be. For effective confining pressure of 100, 200, and 400 kPa, the specimens reached their critical states at deviator stresses of 152, 264, and 434 kPa, respectively. After 28 days of curing, the specimens were tested with the same effective confining pressure, and the results gained were 741, 883, and 1463 kPa, respectively. In terms of deviator stress, the 70 % FA had much higher value compared to the 70 % BA. The deviator stress increased either at peak or critical for both samples, before and after curing, especially for the 70 % FA samples.

After curing time, the particles of the specimens became coarser, as shown in the SEM micrographs. When the confining pressure acted on the specimen, particles came closer, thus resulting in a denser condition. This increased the interlocking between the particles, and the major and the minor effective principle stresses needed higher stress to fail the samples. This led to the deviator stress at failure to become higher too [9,31,32]. Table 4 clearly states the comparison on the result of deviator stress and axial strain at peak, for 30 % FA:70 % BA and 30 % BA:70 % FA specimens with two different curing periods.

The relationship between the deviator stress and the axial strain results in the stiffness of the material. The stress–strain curve is a straight line, and the stiffness is a constant value, obeying the Hooke's law ($\sigma \alpha \varepsilon$). The slope E is presented as the tangent and secant value. The reference point taken for measuring E value is considered at 1 % of the strain value. Comparing the value of E_{sec}, especially after the specimens have undergone 28 days' curing, their E_{sec} values fall between 56.791 and 107.57 MPa. This is similar to the E value of dense sand. Table 5 shows the comparison in secant value of E, to the modulus of elasticity for every specimen. By comparing both 30 and 70 % BA, we get that the E value of 30 % BA is generally higher than that of 70 % BA. According to the range value of soils suggested by (Das 2011), the E_s value gained from these experiments falls in the range of dense sand, which is between 34.4 and 69 MPa.

Based on the results, it seems that the BA content has an effect on the FA–BA mixtures' shear properties. It is found that as the curing days go on, and the pozzolanic process occurs in the sample, this process increases the number of irregularly shaped FA particles, and the particle sizes of FA become coarser. With the increase in internal friction angle, the shear strength of the sample also increases. Based on the

Table 4 Comparison between 30 and 70 % fly ash on deviator stress and axial strain at peak

Effective consolidation pressure (kPa)	0 days				28 days			
	70 % bottom ash		30 % bottom ash		70 % bottom ash		30 % bottom ash	
	Deviator stress at peak, q_p (kPa)	Axial strain at peak, ε_p(%)	Deviator stress at peak, q_p (kPa)	Axial strain at peak, ε_p(%)	Deviator stress at peak, q_p (kPa)	Axial strain at peak, ε_p (%)	Deviator stress at peak, q_p(kPa)	Axial strain at peak, ε_p (%)
100	261	20	242	1.44	566	20	923	2,49
200	334	20	373	2.67	5S7	20	947	LSI
400	662	20	675	2.37	1098	20	1670	2.16

Table 5 Comparison in secant modulus (E_s) for every sample at various curing period

Effective consolidation pressure (kPa)	0 curing clays		28 curing days	
	70 % bottom ash	30 % bottom ash	70 % bottom ash	30 % bottom ash
	E_{secant} (MPa)	E_{secant} (MPa)	E_{secant} (MPa)	E_{secant} (MPa)
100	16.16	20.29	33.31	56.79
200	27.50	34.88	40.20	88.25
400	36.40	63.98	63.02	107.57

Table 6 Comparison between 70 % BA:30 % FA and 30 % BA:70 % FA on shear strength of mixtures at various curing period

Sample	0 curing day			28 curing days		
70 % bottom ash						
Effective consolidation pressure (kPa)	100	200	400	100	200	400
Shear strength (kPa)	130.9	164.8	330.7	280.2	291.7	549.3
30 % bottom ash						
Effective consolidation pressure (kPa)	100	200	400	100	200	400
Shear strength (kPa)	121	186.6	337.5	461.4	474	844.1

results, it is found that the sample with a higher percentage of FA has greater shear strength. This shows that the pozzolanic process of FA plays a crucial role in increasing the strength of the samples. Moreover, effective consolidation pressures acting on the samples also affect their shear strength. The higher the effective consolidation pressure, the more compact and the denser the samples. This is because pore water is being squeezed out. When a sample is denser, the friction between the particles of the samples will increase, thus resulting in the increasing of shear strength [18,33,34]. The results show that the effective consolidation pressure is directly proportional to the shear strength and are presented in Table 6.

Additionally, from Table 6, it seems that for 70 % BA specimens, the shear strength increases by as much as 66–114 %. On the other hand, the percentage shear strength increases for 70 % FA are much higher, i.e., between 150 and 281 %. The results show an apparent comparison between two different ratio mixture specimens, because the ratio of FA in 30 % BA is much higher. The occurrence of pozzolanic reactions for these samples is higher. As observed by SEM micrographs, after 28 days of curing, the ratio of the gel-like product, which binds between the sample particles as a result of pozzolanic reaction, is higher. The particles become coarser, and the interlocking between particles increases the resistance of particles to restrain shearing, thus resulting in greater shear strength [11,35,36].

5 Conclusion

A variety of tests were conducted to identify the morphology, and the chemical and strength characteristics of FA and BA mixtures. Both types of ash were taken from the Tanjung Bin power plant, Johor, Malaysia. The following conclusions can be drawn from this study:

- FA specimens are fine, well rounded, and spherical in shape, with numbers of irregularly shaped particles and smooth particle surfaces. Meanwhile, BA is irregular, rough, and has a gritty surface texture. As the ratio of BA increases, the number of irregular size increases in the mixture. When both of them are mixed, the mixture exhibits some special morphological characteristics that are different from typical sand.
- SEM results indicate that the new cementitious product formed by chemical reaction fill the porous areas inside the mixture, and this leads to a better and stronger aggregate of particles, and finally, a denser mixture is formed. Based on the EDAX results, the new formed gel-like cementitious compounds of C-S-H are believed to be the main cause of this behaviour. In addition, the XRF results show that there is a significant reduction in the elemental ratio of the mixed samples with the increased curing time.
- From engineering point of view, the results of triaxial tests show that the modulus of elasticity of both 30 and 70 % BA mixture fall in the range between 56 and 107 MPa after a 28-day curing period. At both 0 and 28 days of curing, the shear strength of the 70 % BA was higher than that of the 30 % BA. This is a result of the higher interlocking particles of samples with 70 % BA. After 28 days, the samples have pozzolanic activity; hence, the ash particles become coarser and this increases the resistance of particles to restrain the shearing. However, the increase in BA from 30 to 70 % does not have any significant effect on the shear strength characteristic of the FA–BA mixture.

- Results obtained from this study can be used to determine the suitability of FA and BA mixture ratio in geotechnical works, such as soil replacement and soil embankment, or to be used as back-filling material.

Acknowledgments The author wished to acknowledge the financial support given by the Ministry of Science, Technology and Innovation (MOSTI) and Universiti Teknologi Malaysia (UTM) and the support from the Construction Research Alliance and Construction Research Centre UTM.

References

1. Saxena, M.; Asokan, P.; Aparna, A.: Effect of fly ash on clay soil. Clay Res. **17**, 109–114 (1998)
2. Ramadoss, P.; Sundararajan, T.: Utilization of lignite-based bottom ash as partial replacement of fine aggregate in masonry mortar. Arab. J. Sci. Eng. **39**(2), 737–745 (2014)
3. Khan, M.S.; Prasad, J.; Abbas, H.: Effect of high temperature on high-volume fly ash concrete. Arab. J. Sci. Eng. **38**(6), 1369–1378 (2013)
4. Asokan, P.; Saxena, M.; Aparna, A.; Asoletar, S.R.: Characteristics variation of coal combustion residues in an Indian ash pond. Waste Manag. Res. **22**, 265–275 (2004)
5. Canpolat, F.; Yılmaz, K.; Köse, M.M.; Sümer, M.; Yurdusev, M.A.: Use of zeolite, coal bottom ash and fly ash as replacement materials in cement production. Cem. Concr. Res. **34**(5), 731–735 (2004)
6. Chindaprasirt, P.; Jaturapitakkul, C.; Chalee, W.; Rattanasak, U.: Comparative study on the characteristics of fly ash and bottom ash geopolymers. Waste Manag. **29**(2), 539–543 (2009)
7. Naganathan, S.; Subramaniam, N.; Mustapha, K.N.: Development of brick using thermal power plant bottom ash and fly ash. Asian J. Civil Eng. (Building and Housing) **13**, 275–287 (2012)
8. Chindaprasirt, P.; Nuaklong, P.; Zaetang, Y.; Sujumnongtokul, P.; Sata, V.: Mechanical and thermal properties of recycling lightweight pervious concrete. Arab. J. Sci. Eng. **40**, 443–450 (2015)
9. Kaniraj, S.R.; Gayathri, V.: Geotechnical behavior of fly ash mixed with randomly oriented fiber inclusions. Geotext. Geomembr. **21**(3), 123–149 (2003)
10. Pandian, N.S.: Fly ash characterization with reference to geotechnical applications. J. Indian Inst. Sci. **84**(6), 189 (2013)
11. Kutchko, B.G.; Kim, A.G.: Fly ash characterization by SEM–EDS. Fuel **85**(17), 2537–2544 (2006)
12. Pan, J.R.; Huang, C.; Kuo, J.J.; Lin, S.H.: Recycling MSWI bottom and fly ash as raw materials for Portland cement. Waste Manag. **28**(7), 1113–1118 (2008)
13. Targan, Ş.; Olgun, A.; Erdogan, Y.; Sevinc, V.: Influence of natural pozzolan, colemanite ore waste, bottom ash, and fly ash on the properties of Portland cement. Cem. Concr. Res. **33**(8), 1175–1182 (2003)
14. Kou, S.C.; Poon, C.S.; Chan, D.: Influence of fly ash as cement replacement on the properties of recycled aggregate concrete. J. Mater. Civil Eng. **19**(9), 709–717 (2007)
15. Meegoda, J.N.; Gao, S.; Al-Joulani, N.M.A.: Solid waste and ecological issues of coal to energy. J. Hazard. Toxic Radioact. Waste **15**, 99–107 (2011)
16. Bentz, D.P.; Sato, T.; De la Varga, I.; Weiss, W.J.: Fine limestone additions to regulate setting in high volume fly ash mixtures. Cem. Concr. Compos. **34**(1), 11–17 (2012)
17. Kim, B.; Prezzi, M.; Salgado, R.: Geotechnical properties of fly and bottom ash mixtures for use in highway embankments. J. Geotech. Geoenviron. Eng. **131**(7), 914–924 (2005)
18. Sathonsaowaphak, A.; Chindaprasirt, P.; Pimraksa, K.: Workability and strength of lignite bottom ash geopolymer mortar. J. Hazard. Mater. **168**(1), 44–50 (2009)
19. Awang, A.R.; Marto, A.; Makhtar, A.M.: Morphological and strength properties of Tanjung Bin coal ash mixtures for applied in geotechnical engineering work. Int. J. Adv. Sci. Eng. Inf. Technol. **2**, 55–62 (2012)
20. Kathirvel, P.; Saraswathy, V.; Karthik, S.P.; Sekar, A.S.S.: Strength and durability properties of quaternary cement concrete made with fly ash, rice husk ash and limestone powder. Arab. J. Sci. Eng. **38**(3), 589–598 (2013)
21. Muhardi, A.M.; Kassim, K.A.; Makhtar, A.M.; Lee, F.W.; Yap, S.L.: Engineering characteristics of Tanjung Bin coal ash. EJGE **15**, 1117–1129 (2010)
22. Kim, B.J.; Yoon, S.M.; Balunaini, U.: Determination of ash mixture properties and construction of test embankment—part A. Joint Transportation Research Program, Final Report, FHWA/IN/JTRP-2006/24. Purdue University, W. Lafayette, Indiana (2006)
23. Wang, S.; Wu, H.: Environmental-benign utilisation of fly ash as low-cost adsorbents. J. Hazard. Mater. **136**(3), 482–501 (2006)
24. Ginés, O.; Chimenos, J.M.; Vizcarro, A.; Formosa, J.; Rosell, J.R.: Combined use of MSWI bottom ash and fly ash as aggregate in concrete formulation: environmental and mechanical considerations. J. Hazard. Mater. **169**(1), 643–650 (2009)
25. JCPDS: Index to the Powder Diffraction File. International Center for Diffraction Data, Swarthmore (1995)
26. Argiz, C.; Sanjuán, M.A.; Menéndez, E.: Effect of mixes made of coal bottom ash and fly ash on the mechanical strength and porosity of Portland cement. Mater. Constr. **63**(309), 49–64 (2013)
27. Marto, A.; Latifi, N.; Eisazadeh, A.: Effect of non-traditional additives on engineering and microstructural characteristics of laterite soil. Arab. J. Sci. Eng. **39**(10), 6949–6958 (2014)
28. Latifi, N.; Marto, A.; Eisazadeh, A.: Analysis of strength development in non-traditional liquid additive-stabilized laterite soil from macro-and micro-structural considerations. Environ. Earth Sci. **73**, 1133–1141 (2015)
29. Chindaprasirt, P.; De Silva, P.; Hanjitsuwan, S.: Effect of high-speed mixing on properties of high calcium fly ash geopolymer paste. Arab. J. Sci. Eng. **39**, 6001–6007 (2014)
30. Latifi, N.; Eisazadeh, A.; Marto, A.: Strength behavior and microstructural characteristics of tropical laterite soil treated with sodium silicate-based liquid stabilizer. Environ. Earth Sci. **72**, 91–98 (2014)
31. Antiohos, S.; Tsimas, S.: Activation of fly ash cementitious systems in the presence of quicklime: part I. Compressive Strength and pozzolanic reaction rate. Cem. Concr. Res. **34**(5), 769–779 (2004)
32. Eisazadeh, A.; Kassim, K.A.; Nur, H.: Solid-state NMR and FTIR studies of lime stabilized montmorillonitic and lateritic clays. Appl. Clay Sci. **67**, 5–10 (2012)
33. Ghosh, A.; Subbarao, C.: Strength characteristics of class F fly ash modified with lime and gypsum. J. Geotech. Geoenviron. Eng. **133**(7), 757–766 (2007)
34. Marwa, B.A.: Critical State Of Fly Ash–Bottom Ash Mixture. Master Project. Universiti Teknologi Malaysia (2010)
35. Lav, A.H.; Lav, M.A.; Goktepe, A.B.: Analysis and design of a stabilized fly ash as pavement base material. Fuel **85**(16), 2359–2370 (2006)
36. Kaniraj, S.R.; Gayathri, V.: Permeability and consolidation characteristics of compacted fly ash. J. Energy Eng. **130**(1), 18–43 (2004)
37. Head, K.H.; Epps, R.: Manual of Soil Laboratory Testing, vol. 1, pp. 291–298. Pentech Press, London (1980)
38. Das, B.M.: Principles of Foundation Engineering, 7th edn. Cengage Learning, Boston (2011)